
Figures and figure supplements

A *Ctnnb1* enhancer transcriptionally regulates Wnt signaling dosage to balance homeostasis and tumorigenesis of intestinal epithelia

Xiaojiao Hua et al.

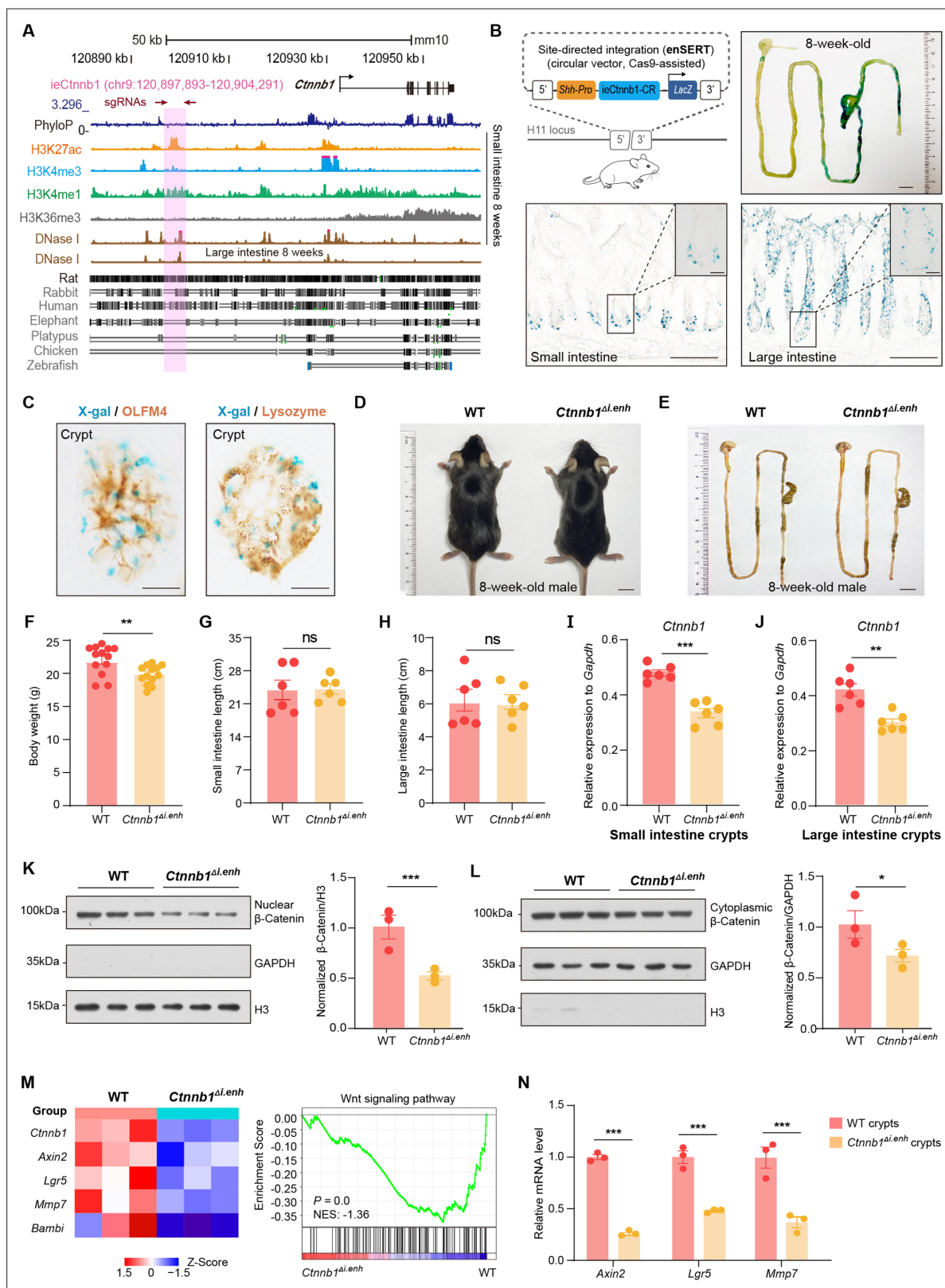


Figure 1. ieCtnnb1 is an intestinal enhancer of *Ctnnb1*. **(A)** Schematic representation of the upstream region of mouse *Ctnnb1* gene and the location of ieCtnnb1 (6,399 bp, pink shading), which is marked by H3K27ac and H3K4me1 peaks, and DNase I hypersensitivity in small intestine and large intestine of 8-week-old mice. The sequence conservation of the indicated species is shown at the bottom as vertical lines. Data were obtained from ENCODE. Locations of single-guide RNAs (sgRNAs) for generating ieCtnnb1 knockout mice were marked. **(B)** Top left: a schematic illustration showing that the

Figure 1 continued on next page

Figure 1 continued

knock-in reporter construct carries the *Shh* promoter, ieCtnnb1 core region sequences (2,153 bp), and the *LacZ* reporter gene. Top right: X-Gal staining (blue) of the gastrointestinal (GI) tract of an 8-week-old *H11^{i,enh}* mouse. Bottom: X-Gal staining (blue) of the small intestine (left) and colon (right) of an 8-week-old *H11^{i,enh}* mouse. Boxed areas were enlarged at top-right corners. (C) Representative images of small intestinal crypts co-labeled by X-Gal with OLFM4 (left), and X-Gal with Lysozyme (right). (D–E) Representative images of whole body (d) and GIs (e) of 8-week-old male wildtype (WT) and *Ctnnb1^{Δi,enh}* mice. (F) Comparison of the body weight of 8-week-old male WT (n=13) and *Ctnnb1^{Δi,enh}* (n=13) mice. (G–H) Measurements of small (G) and large (H) intestine length of 8-week-old male WT (n=6) and *Ctnnb1^{Δi,enh}* (n=6) mice. (I–J) Relative mRNA levels of *Ctnnb1* in small (I) and large (J) intestinal crypts of WT (n=6) and *Ctnnb1^{Δi,enh}* (n=6) mice. (K–L) Left: immunoblotting of nuclear (K) and cytoplasmic (L) β-catenin, GAPDH, and H3 of small intestinal crypts of WT (n=3) and *Ctnnb1^{Δi,enh}* (n=3) mice. Right: histograms showing protein levels of β-catenin normalized to H3 (K) or GAPDH (L) levels. Values of WT were set as '1'. (M) Heatmap of indicated Wnt target genes and gene set enrichment analysis (GSEA) of Wnt signaling pathway according to transcriptome profiles of small intestinal crypts of WT (n=3) and *Ctnnb1^{Δi,enh}* (n=3) mice. (N) Quantitative reverse transcription PCR (RT-qPCR) showing relative mRNA levels of indicated Wnt target genes (*Axin2*, *Lgr5*, and *Mmp7*) in small intestinal crypts of WT (n=3) and *Ctnnb1^{Δi,enh}* (n=3) mice. Scale bars, 1 cm (B, top; D and E), 100 μm (B, bottom), 10 μm (B, magnified views; C). Quantification data are shown as means ± SEM, statistical significance was determined using an unpaired two-tailed Student's t-test (F–L). Quantification data are shown as means ± SD, statistical significance was determined using Multiple t-tests – one per row (N). *p<0.05, **p<0.01, ***p<0.001, and ****p<0.0001. ns, not significant. NES: normalized enrichment score.

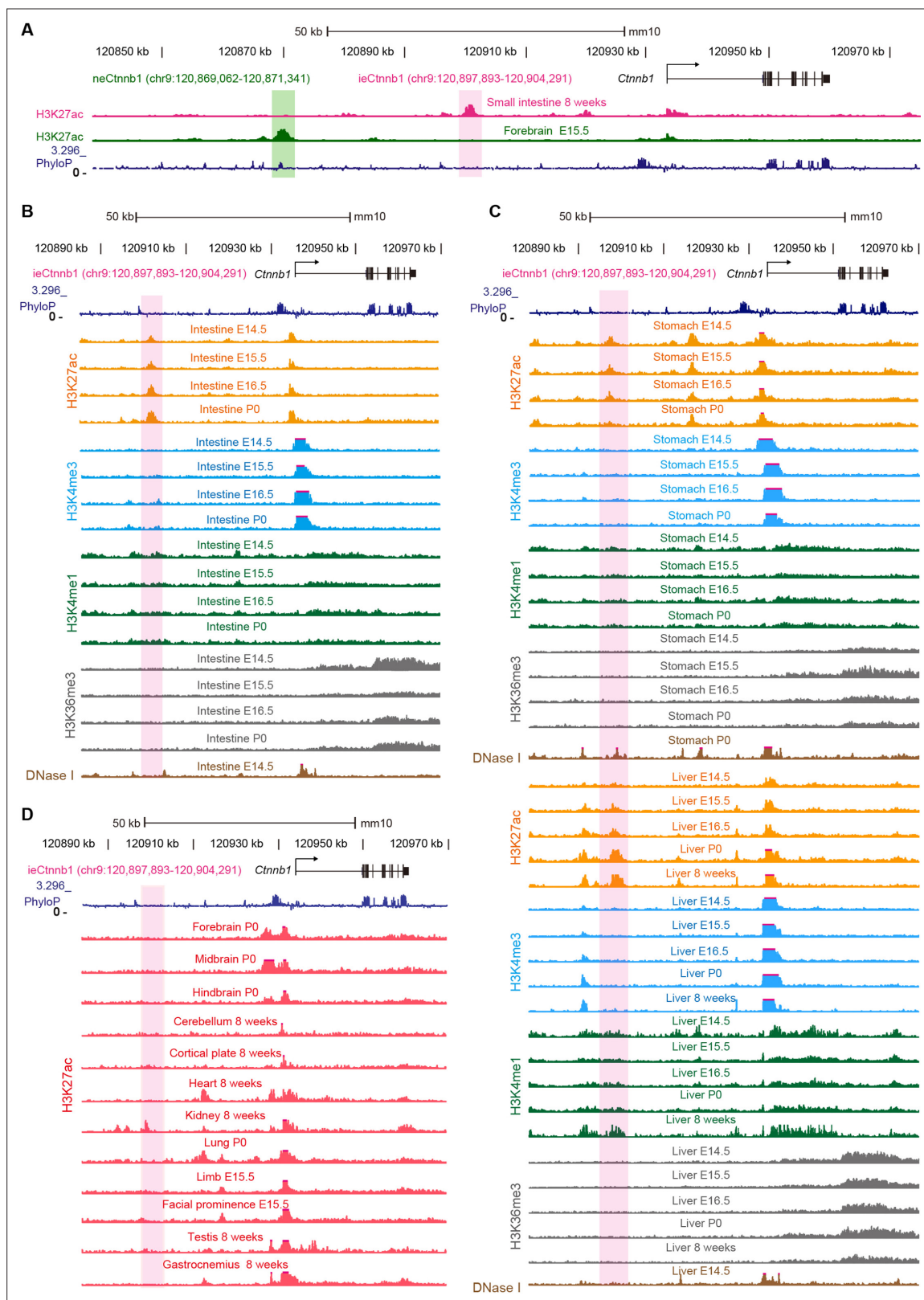


Figure 1—figure supplement 1. *ieCtnnb1* is a putative intestinal enhancer upstream of *Ctnnb1*. **(A)** Schematic representation of the upstream region of mouse *Ctnnb1* gene and locations of enhancer *neCtnnb1* (green shading) and putative enhancer *ieCtnnb1* (pink shading). Data were obtained from ENCODE. **(B–C)** Enrichment of indicated signals in developing intestine **(B)**, stomach, and liver **(C)** were shown. Data were obtained from ENCODE. **(D)** Enrichment of H3K27ac chromatin immunoprecipitation sequencing (ChIP-seq) signals in indicated mouse tissues. Data were obtained from ENCODE.

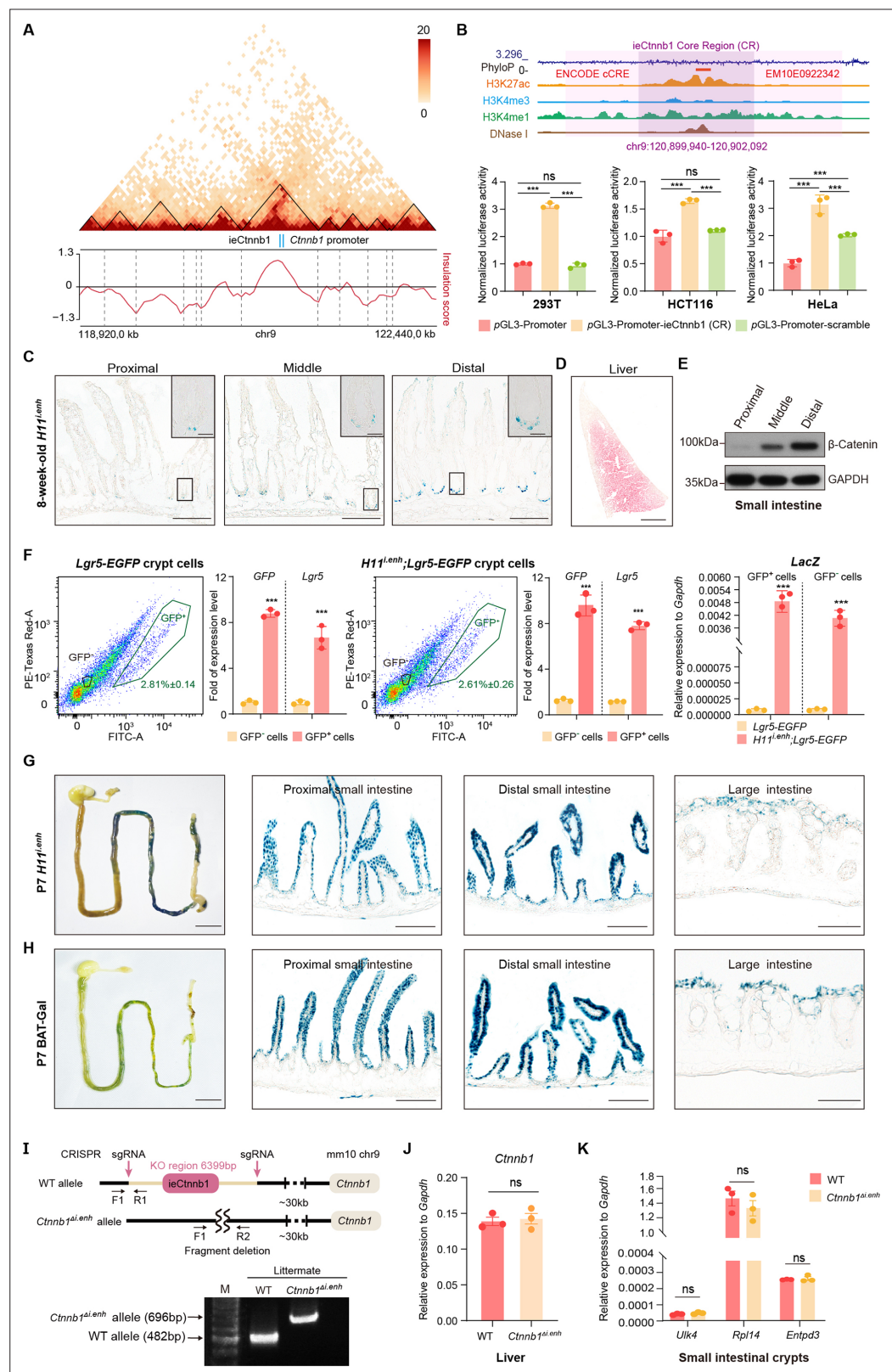


Figure 1—figure supplement 2. ieCtnnb1 is predominantly active in developing intestine. **(A)** Hi-C data of BALB/c mouse large intestine at indicated locus. Boundaries of topologically associating domains (TADs) and locations of *Ctnnb1* promoter and ieCtnnb1 (blue bars) were marked. **(B)** Top: schematic representation of ieCtnnb1 core region (2,153 bp, dark purple shading). The location of an annotated ENCODE cCRE was marked. Figure 1—figure supplement 2 continued on next page

Figure 1—figure supplement 2 continued

indicated. Bottom: HEK293T, HCT116, and HeLa cells were transfected with indicated plasmids for 48 hr for luciferase reporter assay. **(C)** Representative images showing X-Gal staining of proximal, middle, and distal small intestinal sections of 8-week-old *H11^{l.enh}* mice (blue). **(D)** Representative image showing X-Gal and eosin staining of the liver of 8-week-old *H11^{l.enh}* mice (X-Gal: blue, eosin: red). **(E)** Immunoblotting of indicated proteins derived from proximal, middle, and distal small intestine tissues of WT C57/BL6 mice. **(F)** Flow cytometry assays to isolate GFP+ and GFP- cells from small intestinal crypts of *Lgr5*-EGFP (n=3) and *Ctnnb1^{Δi.enh}*; *Lgr5*-EGFP (n=3) mice. Quantitative reverse transcription PCR (RT-qPCR) showing relative mRNA levels of *GFP*, *Lgr5*, and *LacZ* in aforementioned GFP+ and GFP- cells. **(G–H)** Representative images showing X-Gal staining of gastrointestinal tracts, and sections of proximal and distal small intestine, and large intestine of P7 *H11^{l.enh}* **(G)** mice and P7 BAT-Gal mice **(H)**. **(I)** Generation and genotyping of *Ctnnb1^{Δi.enh}* mice. WT, wild-type; sgRNA, single-guide RNA. **(J)** Relative mRNA levels of *Ctnnb1* in the liver of WT (n=3) and *Ctnnb1^{Δi.enh}* (n=3) mice. **(K)** Relative mRNA levels of genes (*Ulk4*, *Rpl14*, and *Entpd3*) located in the same TAD as *Ctnnb1* in small intestinal crypts of WT (n=3) and *Ctnnb1^{Δi.enh}* (n=3) mice. Scale bars, 1 cm (whole mount in F and G), 100 μm (**C**, **D**, **F**, and **G**), 10 μm (magnified insets in C). Quantification data are shown as means ± SEM. Statistical significance was determined using two-way ANOVA **(B)** and an unpaired two-tailed Student's *t*-test (**F**, **J**, and **K**). *p<0.05, **p<0.01, ***p<0.001, and ****p<0.0001. ns, not significant.

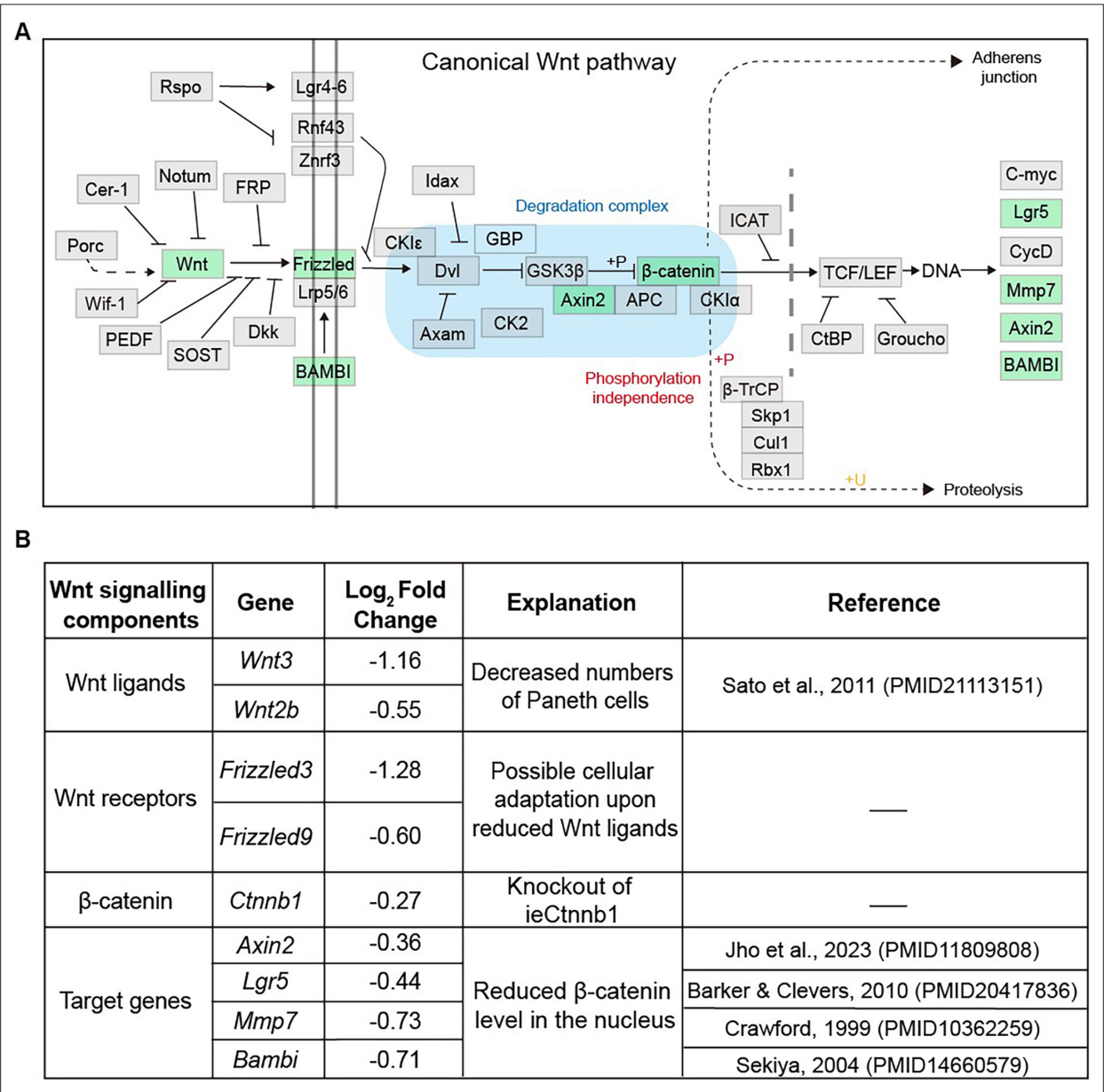


Figure 1—figure supplement 3. The list of Wnt signaling pathway components downregulated in *Ctnnb1^{Δi.enh}* crypts. **(A)** A schematic diagram highlighting downregulated components of the Wnt signaling pathway in the crypts of the *Ctnnb1^{Δi.enh}* small intestine. **(B)** A table showing Wnt signaling pathway components downregulated in *Ctnnb1^{Δi.enh}* crypts.

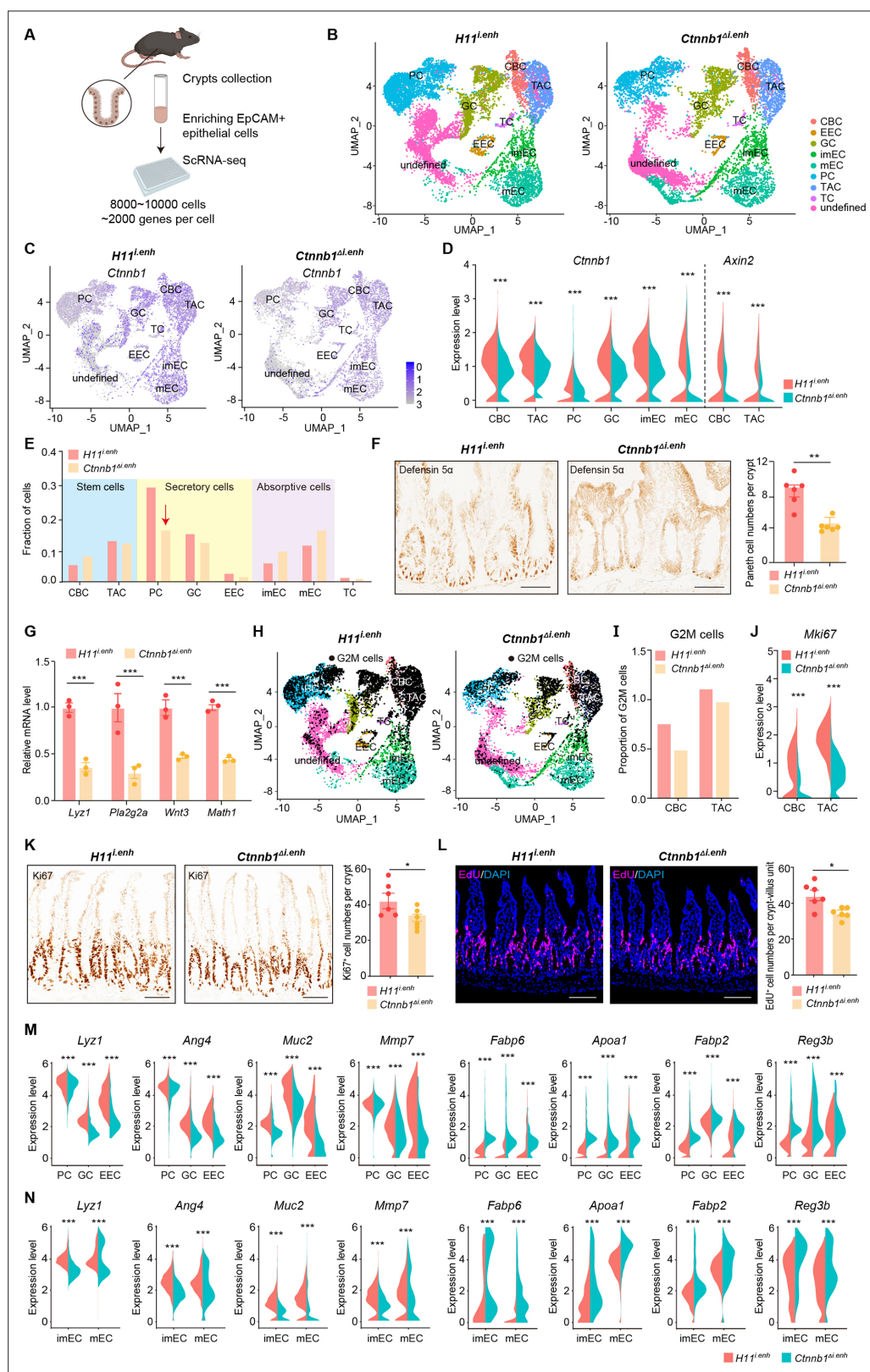


Figure 2. ieCtnnb1 knockout altered cellular composition and expression profiles of small intestinal crypts. (A) Schematic illustration of single-cell sequencing. Crypts were extracted from small intestines followed by fluorescence activated cell sorting (FACS) to enrich EpCAM+ DAPI- epithelial cells. Cells of two 10-week-old female mice for each genotype were pooled together to perform single-cell transcriptome analyses. (B) Uniform

Figure 2 continued on next page

Figure 2 continued

Manifold Approximation and Projection (UMAP) were used to visualize the clustering of 11,824 single cells from *H11^{i.enh}* mice and 8,094 single cells from *Ctnnb1^{Δi.enh}* mice. Cell types were assigned according to expressions of marker genes. CBC, crypt base columnar cell; TAC, transit-amplifying cell; EEC, enteroendocrine cell; imEC, immature enterocytes; mEC, mature enterocytes; GC, goblet cell; PC, Paneth cell; TC, tuft cell. **(C)** Expression and distribution of *Ctnnb1* in small intestinal crypt cells of *H11^{i.enh}* and *Ctnnb1^{Δi.enh}* mice. **(D)** Violin plots showing the expression of *Ctnnb1* in CBC, TAC, PC, GC, imEC, mEC; and the expression of *Axin2* in CBC and TAC, of *H11^{i.enh}* and *Ctnnb1^{Δi.enh}* mice. **(E)** Comparison of the proportion of indicated small intestinal crypt cell types in *H11^{i.enh}* and *Ctnnb1^{Δi.enh}* mice. **(F)** Immunohistochemistry (left and middle) and quantification (right) of PCs in small intestines of *H11^{i.enh}* (n=6) and *Ctnnb1^{Δi.enh}* (n=6) mice. **(G)** Quantitative reverse transcription PCR (RT-qPCR) showing relative mRNA levels of PC marker genes (*Lyz1*, *Pla2g2a*, *Wnt3*, *Math1*) in small intestinal crypts of *H11^{i.enh}* (n=3) and *Ctnnb1^{Δi.enh}* (n=3) mice. **(H)** Distribution of G2M cells in *H11^{i.enh}* and *Ctnnb1^{Δi.enh}* small intestinal crypts, based on the expression of cell cycle marker gene *Mki67*. **(I)** Comparison of the proportion of G2M cells in CBC and TAC of *H11^{i.enh}* and *Ctnnb1^{Δi.enh}* small intestinal crypts. **(J)** Violin plots showing the expression of *Mki67* in CBC and TAC of *H11^{i.enh}* and *Ctnnb1^{Δi.enh}* small intestinal crypts. **(K)** Immunohistochemistry (left and middle) and quantification (right) of Ki67+ cells in small intestines of *H11^{i.enh}* (n=6) and *Ctnnb1^{Δi.enh}* (n=6) mice. **(L)** Immunofluorescence (left and middle) and quantification (right) of EdU+ cells (red) in small intestines of *H11^{i.enh}* (n=6) and *Ctnnb1^{Δi.enh}* (n=6) mice after 4 hr EdU injection. Nuclei were labeled with DAPI (blue). **(M–N)** Violin plots showing expressions of marker genes for secretory cells (*Lyz1*, *Ang4*, *Muc2*, *Mmp7*) and absorptive cells (*Fabp6*, *Apoa1*, *Fabp2*, *Reg3b*) in secretory(M) and absorptive lineages (N) of *H11^{i.enh}* and *Ctnnb1^{Δi.enh}* small intestinal crypts. Scale bars, 50 μm (F, K, and L). Quantification data are shown as means ± SEM, statistical significance was determined using an unpaired two-tailed Student's t-test (D, F, J, K, L, M, and N). Quantification data are shown as means ± SD, statistical significance was determined using Multiple t-tests – one per row (G). *p<0.05, **p<0.01, ***p<0.001, and ****p<0.0001. ns, not significant.

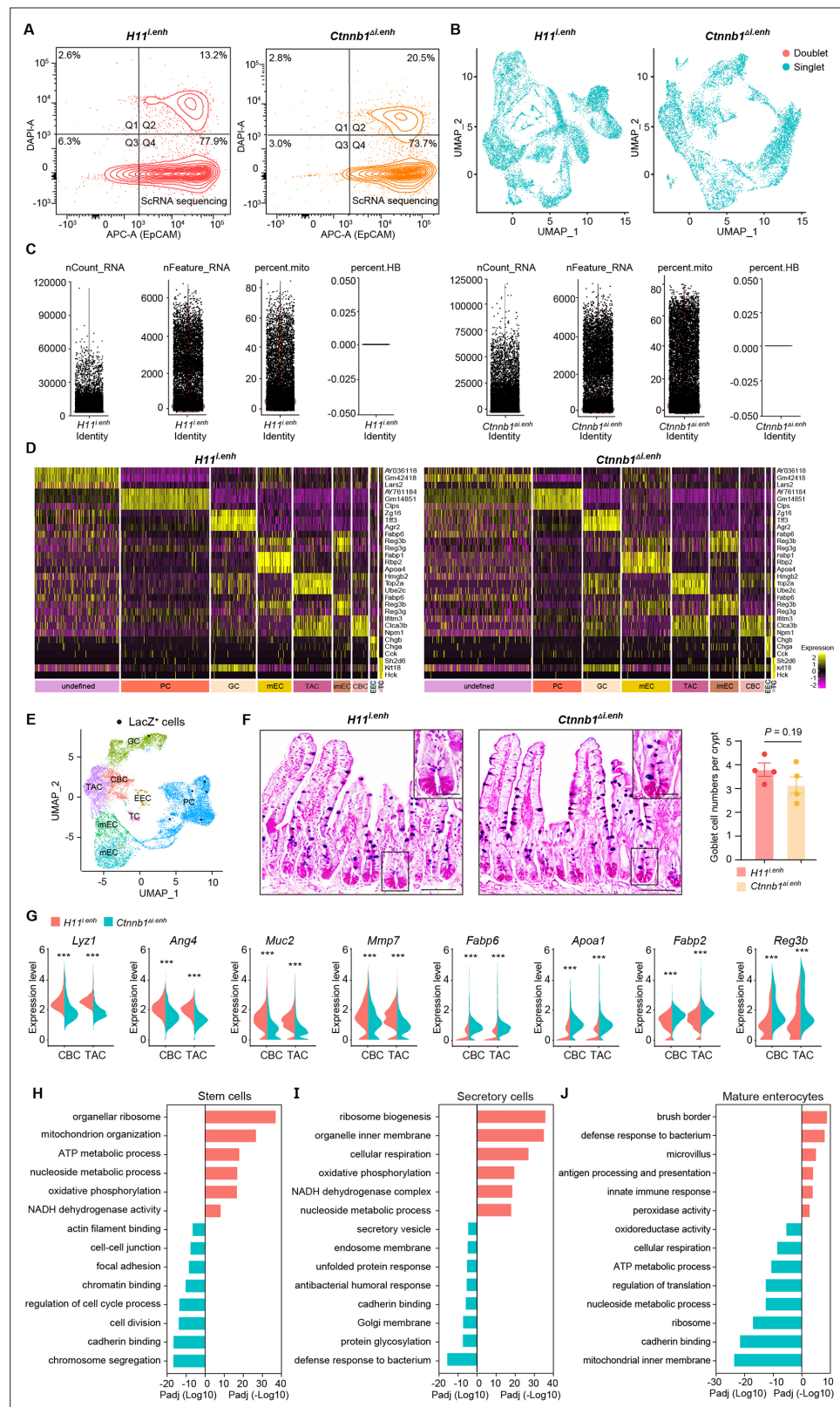


Figure 2—figure supplement 1. Single-cell survey of small intestinal crypt cells upon ieCtnnb1 knockout. (A) Flow cytometry assays for isolating EpCAM⁺ DAPI⁺ epithelial cells from *H1^{fl/enh}* (n=2) and *Ctnnb1^{Δi/enh}* (n=2) small intestinal crypts. (B) Results of cell filtration using DoubletFinder. 1,294 doublets of 11,824 cells from *H1^{fl/enh}* crypts and 567 doublets of 8,094 cells from *Ctnnb1^{Δi/enh}* crypts were identified (blue dots: singlets, red dots: doublets).

Figure 2—figure supplement 1 continued on next page

Figure 2—figure supplement 1 continued

doublings). (C) Results of cell filtration using Seurat. Cells with more than 30% of reads derived from mitochondrial genes are considered dead and removed from the analysis. (D) Cell-type-specific signatures. Heatmap showing relative expression levels (row-wise Z scores) of genes (rows) in cell-type-specific signatures. (E) Uniform Manifold Approximation and Projection (UMAP) visualizing LacZ+ single cells (black dots) of *H11^{i.enh}* small intestinal crypts (n=4 mice). (F) Alcian Blue PAS staining and quantification of goblet cells in the small intestine of *H11^{i.enh}* (n=6) and *Ctnnb1^{Δi.enh}* (n=6) mice. (G) Violin plots showing expressions of marker genes for secretory cells (*Lyz1*, *Ang4*, *Muc2*, *Mmp7*) and absorptive cells (*Fabp6*, *Apoa1*, *Fabp2*, *Reg3b*) in *H11^{i.enh}* and *Ctnnb1^{Δi.enh}* crypt base columnar (CBCs) and transit-amplifying cells (TACs). (H–J) Gene ontology (GO) analysis of differential genes in stem cell lineage (H), secretory lineage (I), and mature enterocytes (J) of *H11^{i.enh}* and *Ctnnb1^{Δi.enh}* crypts. Scale bars, 50 μm (E), 10 μm (magnified views in E). Quantification data are shown as means ± SEM, statistical significance was determined using an unpaired two-tailed Student's t-test (F and G). *p<0.05, **p<0.01, ***p<0.001, and ****p<0.0001. ns, not significant.

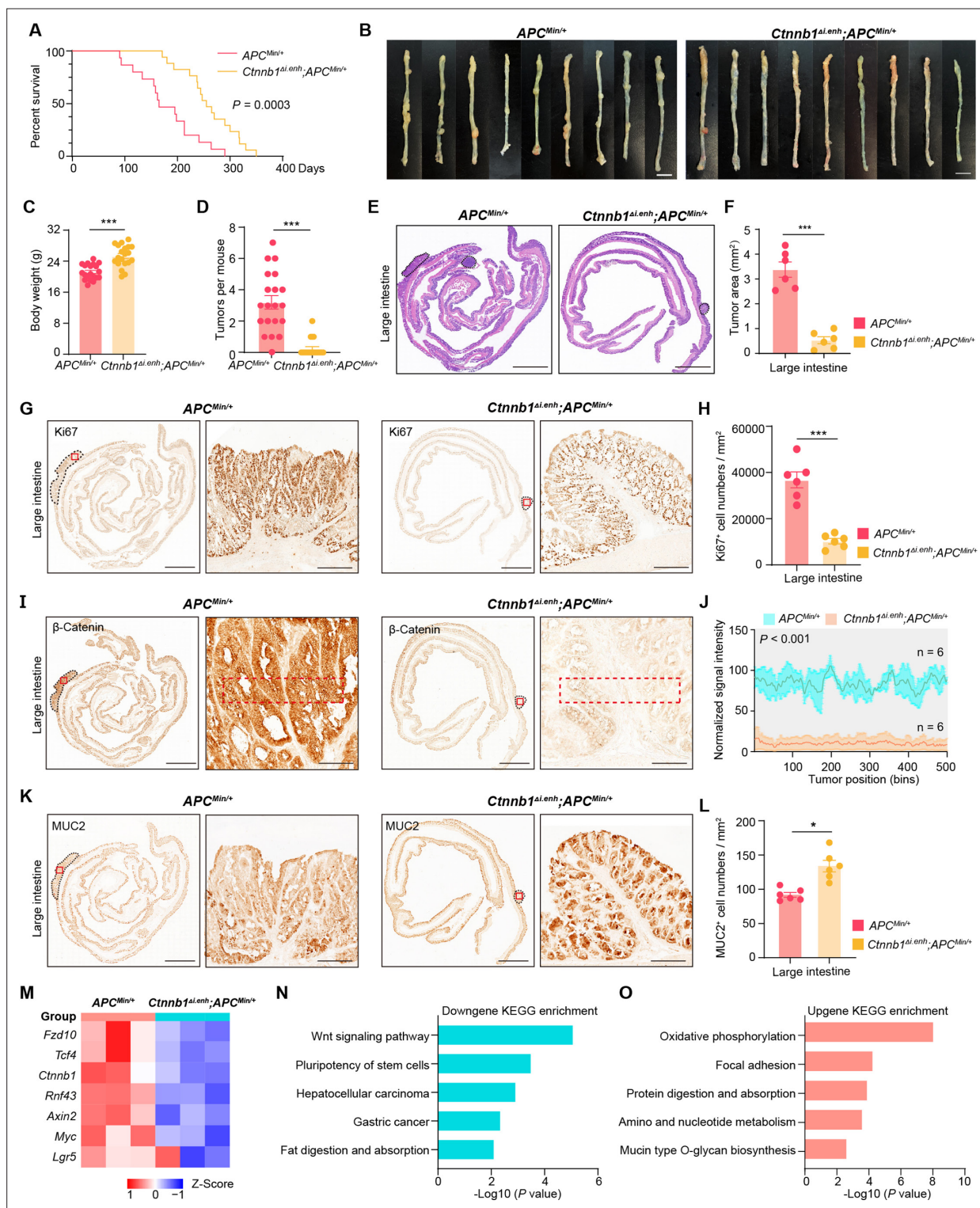


Figure 3. Knocking out ieCtnnb1 inhibits tumorigenesis of colorectal cancer. (A) Survival of $Apc^{Min/+}$ ($n=15$) and $Ctnnb1^{\Delta i.enh};Apc^{Min/+}$ ($n=17$) mice. (B) Colon images of 5-month-old $Apc^{Min/+}$ ($n=9$) and $Ctnnb1^{\Delta i.enh};Apc^{Min/+}$ ($n=9$) mice. (C) Weight statistics of 5-month-old $Apc^{Min/+}$ ($n=20$) and $Ctnnb1^{\Delta i.enh};Apc^{Min/+}$ ($n=20$) mice. (D) The statistical analysis of tumor counts in colons of 5-month-old $Apc^{Min/+}$ ($n=9$) and $Ctnnb1^{\Delta i.enh};Apc^{Min/+}$ ($n=9$) mice. (E) Representative H&E staining images of colon sections of 5-month-old $Apc^{Min/+}$ and $Ctnnb1^{\Delta i.enh};Apc^{Min/+}$ mice. (F) The statistical analysis of colon tumor area in 5-month-old $Apc^{Min/+}$ ($n=6$) and $Ctnnb1^{\Delta i.enh};Apc^{Min/+}$ ($n=6$) mice. (G–H) Immunohistochemistry (G) and quantification (H) of Ki67+ cells in colon tumors of 5-month-old $Apc^{Min/+}$ ($n=6$) and $Ctnnb1^{\Delta i.enh};Apc^{Min/+}$ ($n=6$) mice. (I–J) Immunohistochemistry (I) and signal intensity statistics (J, red dashed boxes of I) of β-catenin in colon tumors of 5-month-old $Apc^{Min/+}$ ($n=6$) and $Ctnnb1^{\Delta i.enh};Apc^{Min/+}$ ($n=6$) mice. (K–L) Immunohistochemistry (K) and quantification (L) of MUC2+ cells in colon tumors of 5-month-old $Apc^{Min/+}$ ($n=6$) and $Ctnnb1^{\Delta i.enh};Apc^{Min/+}$ ($n=6$) mice. (M) Heatmap of Z-score for gene expression analysis. (N) Bar graph of downgene KEGG enrichment for $Apc^{Min/+}$ mice. (O) Bar graph of upgene KEGG enrichment for $Ctnnb1^{\Delta i.enh};Apc^{Min/+}$ mice.

Figure 3 continued on next page

Figure 3 continued

quantification (**L**) of MUC2+ cells in colon tumors of 5-month-old *Apc*^{Min/+} (n=6) and *Ctnnb1*^{Δi.enh};*Apc*^{Min/+} (n=6) mice. (**M**) The heatmap showing relative expressions of Wnt signaling pathway genes of colon tumors from 5-month-old *Apc*^{Min/+} (n=3) and *Ctnnb1*^{Δi.enh};*Apc*^{Min/+} (n=3) mice. (**N–O**) KEGG analyses of downregulated (**N**) and upregulated (**O**) genes in colon tumors of 5-month-old *Apc*^{Min/+} (n=3) and *Ctnnb1*^{Δi.enh};*Apc*^{Min/+} (n=3) mice. Scale bars, 1 cm (**B**), 4 mm (**E, G, I, and K**), 200 μm (magnified views in G and K), 100 μm (magnified views in I). Quantification data are shown as means ± SEM, statistical significance was determined using an unpaired two-tailed Student's t-test (**C, D, F, H, J, and L**) or log-rank analysis (**A**). *p<0.05, **p<0.01, ***p<0.001, and ****p<0.0001. ns, not significant.

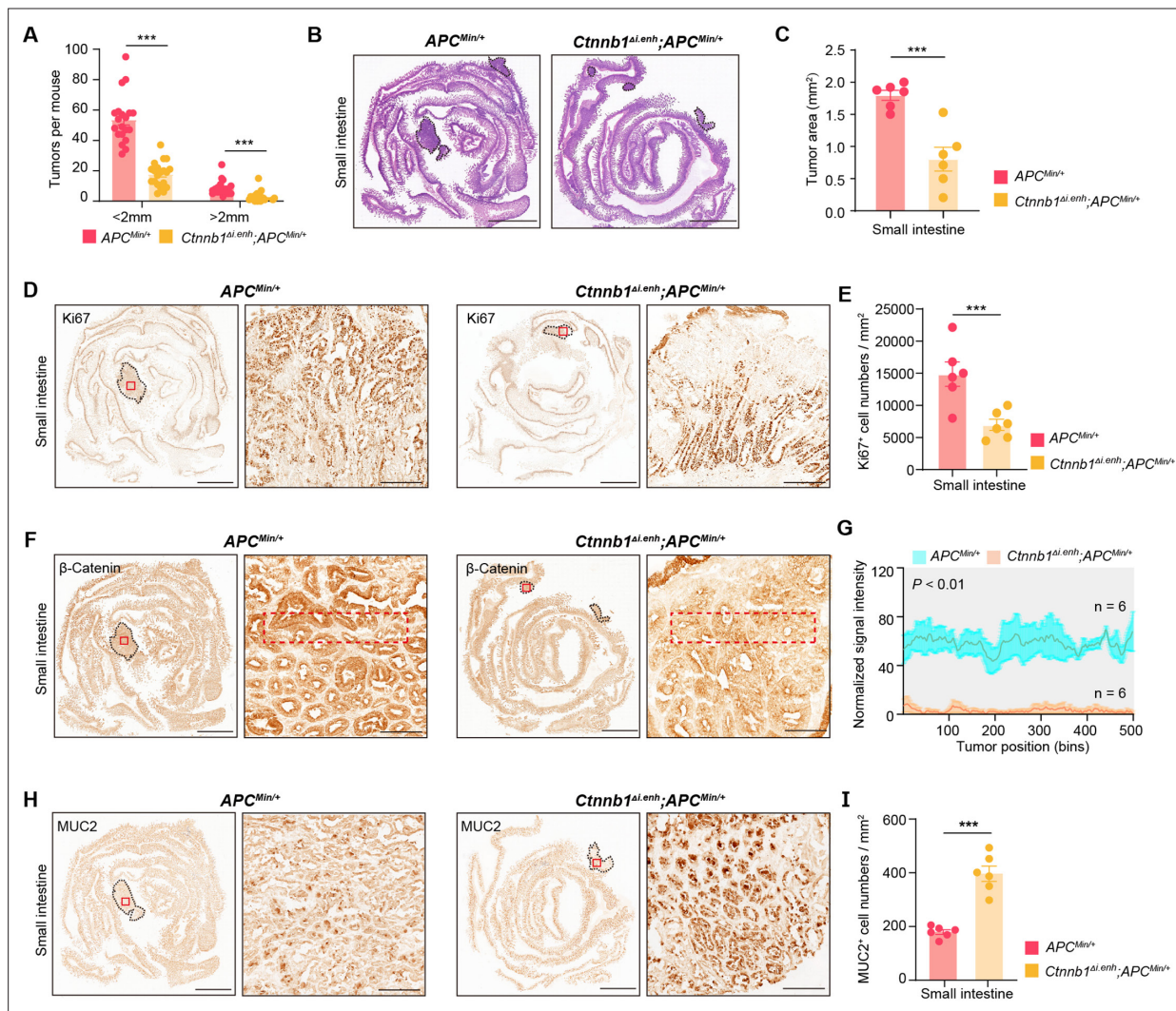


Figure 3—figure supplement 1. Knocking out ieCtnnb1 inhibits tumorigenesis of small intestine. (A) Statistical analyses of tumor counts in small intestines of 5-month-old *Apc*^{Min/+} (n=20) and *Ctnnb1*^{Δi.enh};*Apc*^{Min/+} (n=20) mice. (B) Representative H&E staining images of small intestine sections of 5-month-old *Apc*^{Min/+} and *Ctnnb1*^{Δi.enh};*Apc*^{Min/+} mice. (C) The statistical analysis of small intestinal tumor area in 5-month-old *Apc*^{Min/+} (n=6) and *Ctnnb1*^{Δi.enh};*Apc*^{Min/+} (n=6) mice. (D–E) Immunohistochemistry (D) and quantification (E) of Ki67+ cells in small intestinal tumors of 5-month-old *Apc*^{Min/+} (n=6) and *Ctnnb1*^{Δi.enh};*Apc*^{Min/+} (n=6) mice. (F–G) Immunohistochemistry (F) and signal intensity statistics (G, red dashed boxes of F) of β-catenin in small intestinal tumors of 5-month-old *Apc*^{Min/+} (n=6) and *Ctnnb1*^{Δi.enh};*Apc*^{Min/+} (n=6) mice. (H–I) Immunohistochemistry (H) and quantification (I) of MUC2+ cells in small intestinal tumors of 5-month-old *Apc*^{Min/+} (n=6) and *Ctnnb1*^{Δi.enh};*Apc*^{Min/+} (n=6) mice. Scale bars, 4 mm (B, D, F, and H), 200 μm (magnified views in D and H), 100 μm (magnified views in F). Quantification data are shown as means ± SEM, statistical significance was determined using an unpaired two-tailed Student's t-test (C, E, G, and I) or Multiple t-tests – one per row (A). *p<0.05, **p<0.01, ***p<0.001, and ****p<0.0001. ns, not significant.

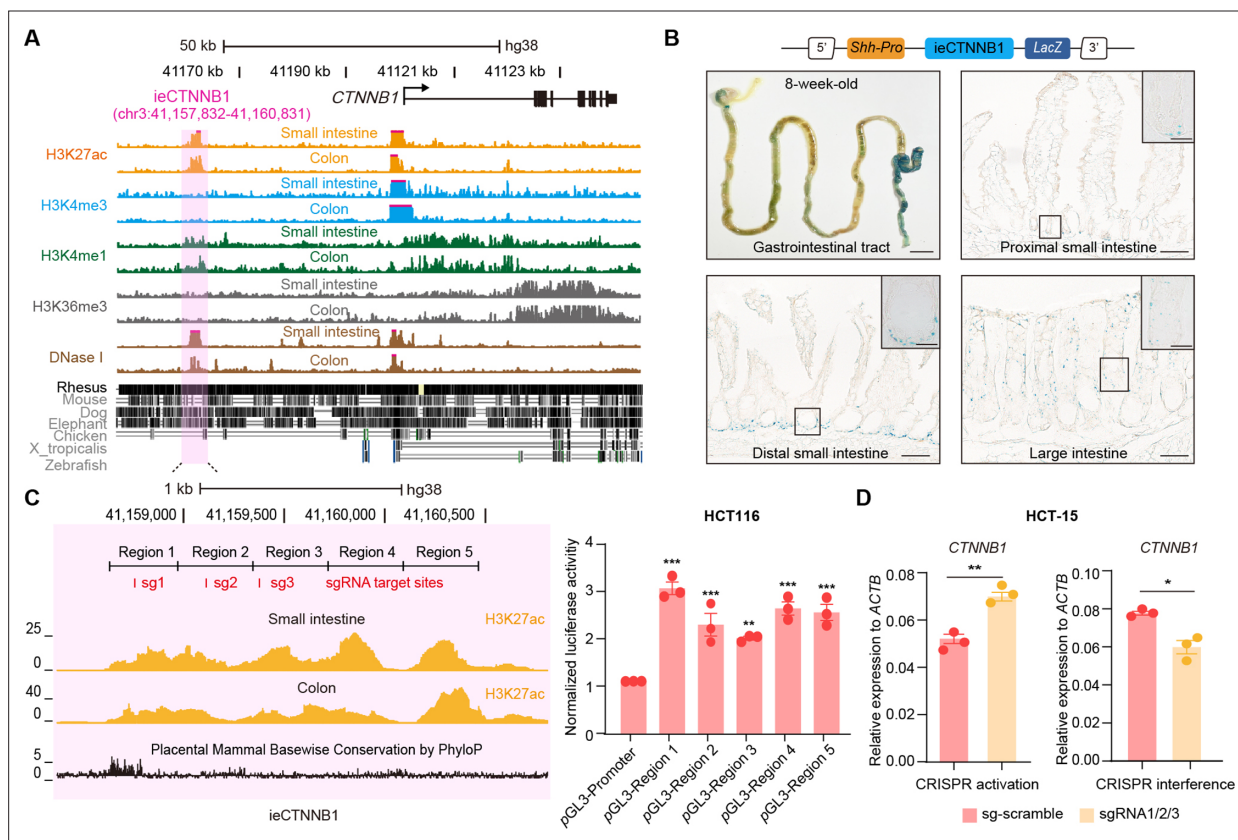


Figure 4. ieCTNNB1 is the intestinal enhancer of human *CTNNB1*. **(A)** Schematic representation of human *CTNNB1* gene and the location of ieCTNNB1 (3,000 bp, pink shading), which is marked by H3K27ac and H3K4me1 peaks, and DNaseI hypersensitivity in human small intestine (30-year-old female) and colon (34-year-old male). Data were obtained from ENCODE. **(B)** Top: a schematic illustration showing that the knock-in construct containing the *Shh* promoter, ieCTNNB1 sequences (3,000 bp), and the *LacZ* reporter gene. Bottom: X-Gal staining (blue) of the gastrointestinal tract, and sections of the proximal small intestine, distal small intestine, and large intestine in 8-week-old *H11^{hi.enh}* mice. **(C)** Left: ieCTNNB1 is marked by enrichment of H3K27ac in human small intestine (30-year-old female) and colon (34-year-old male). Data were obtained from ENCODE. Locations of single-guide RNA (sgRNA) target sites were indicated. Five subregions of ieCTNNB1 were shown. Right: luciferase reporter assay in HCT116 cells transfected with indicated plasmids for 48 hr. **(D)** Quantitative reverse transcription PCR (RT-qPCR) showing relative mRNA levels of *CTNNB1* in HCT-15 cells transfected with indicated CRISPR activation or CRISPR interference vectors for 48 hr. Scale bars, 1 cm (whole mount in B), 100 μ m (sections in B), 10 μ m (magnified views in B). Quantification data are shown as means \pm SEM, statistical significance was determined using one-way ANOVA (**C**) and an unpaired two-tailed Student's *t*-test (**D**). **p*<0.05, ***p*<0.01, ****p*<0.001, and *****p*<0.0001. ns, not significant.

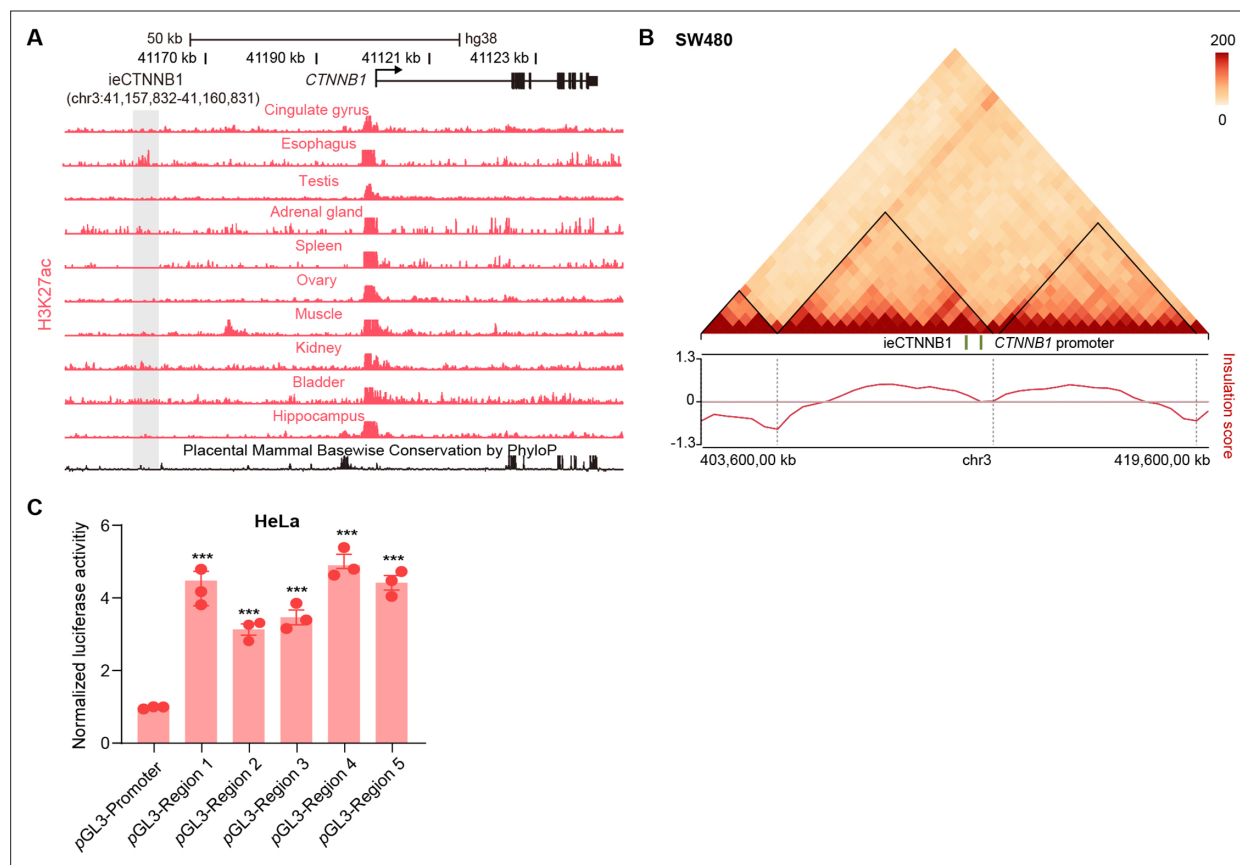


Figure 4—figure supplement 1. ieCTNNB1 is the intestinal enhancer of human *CTNNB1*. **(A)** Schematic representation of the upstream region of human *CTNNB1* gene and the location of ieCTNNB1 (gray shading). Enrichment of H3K27ac chromatin immunoprecipitation sequencing (ChIP-seq) signals in indicated human tissues was shown. Data were obtained from ENCODE. **(B)** Hi-C data of SW480 cells. Boundaries of the topologically associating domains (TADs) and locations of *CTNNB1* promoter and ieCTNNB1 (green bar) were marked. **(C)** Luciferase reporter assays of HeLa cells transfected with indicated plasmids for 48 hr. Quantification data are shown as means \pm SEM, statistical significance was determined using one-way ANOVA. **(C)**. * $p < 0.05$, ** $p < 0.01$, *** $p < 0.001$, and **** $p < 0.0001$. ns, not significant.

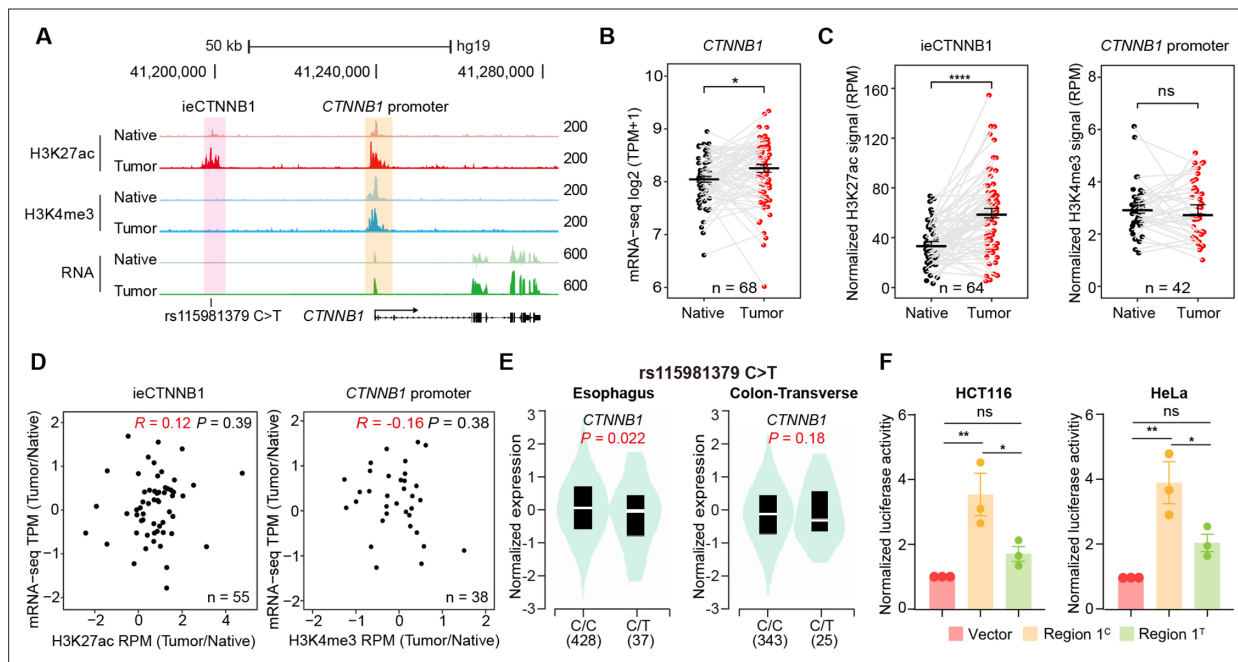


Figure 5. ieCTNNB1 is activated in colorectal cancer and its activity positively correlates with the expression of CTNNB1. **(A)** Schematic representation of ieCTNNB1 (pink shading) and CTNNB1 promoter (yellow shading), which is respectively marked by H3K27ac and H3K4me3 peaks, and mRNA signals in native and tumor tissues of a patient with colorectal cancer. The location of risk mutation site was indicated. **(B)** Comparison of CTNNB1 expression levels in native and tumor tissues of colorectal cancer patients (n=68). **(C)** Left: comparison of H3K27ac signals at ieCTNNB1 in native and tumor tissues of colorectal cancer patients (n=64). Right: comparison of H3K4me3 signals at CTNNB1 promoter in native and tumor tissues of colorectal cancer patients (n=42). **(D)** Left: correlation between H3K27ac signals at ieCTNNB1 and CTNNB1 expression in native and tumor tissues of colorectal cancer patients (n=55). Right: correlation between H3K4me3 signals at CTNNB1 promoter and CTNNB1 expression in native and tumor tissues of colorectal cancer patients (n=38). **(E)** Left: comparison of CTNNB1 expression in esophagus between subjects with common sequence (C/C, n=428) and variant sequence (C/T, n=37). Right: comparison of CTNNB1 expression in transverse colon between subjects with common sequence (C/C, n=343) and variant sequence (C/T, n=25). **(F)** Luciferase reporter assay in HCT116 and HeLa cells transfected with indicated plasmids for 48 hr. Quantification data are shown as means \pm SEM, statistical significance was determined using a paired (B, C, and D) or unpaired (E) two-tailed Student's t-test and two-way ANOVA (F). *p<0.05, **p<0.01, ***p<0.001, and ****p<0.0001. ns, not significant. R: Pearson correlation.

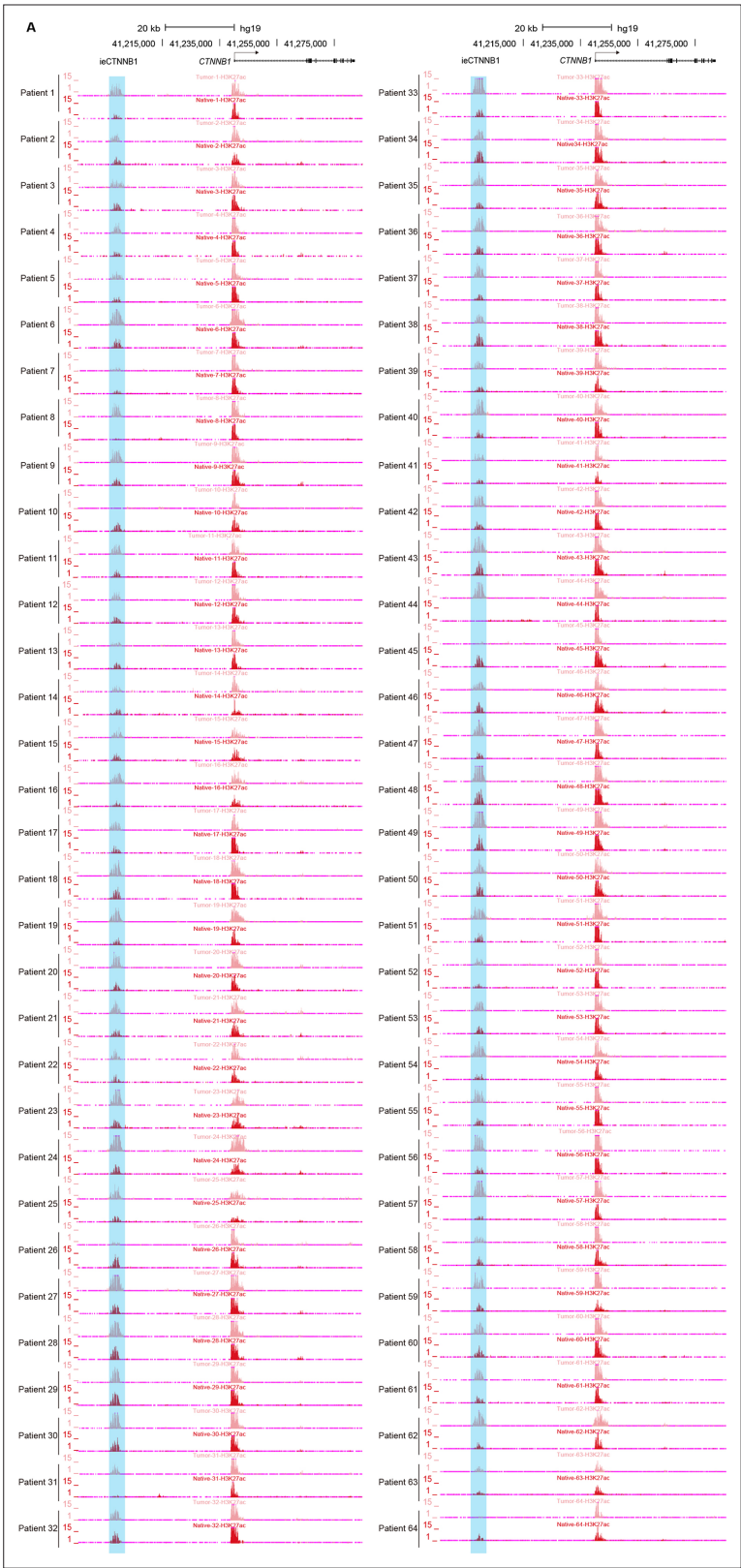


Figure 5—figure supplement 1. *ieCTNNB1* is activated in colorectal cancer. **(A)** H3K27ac chromatin immunoprecipitation sequencing (ChIP-seq) signals at *ieCTNNB1* (blue shading) in paired tumor (top) and native (bottom) tissues of patients with colorectal cancer (n=64).

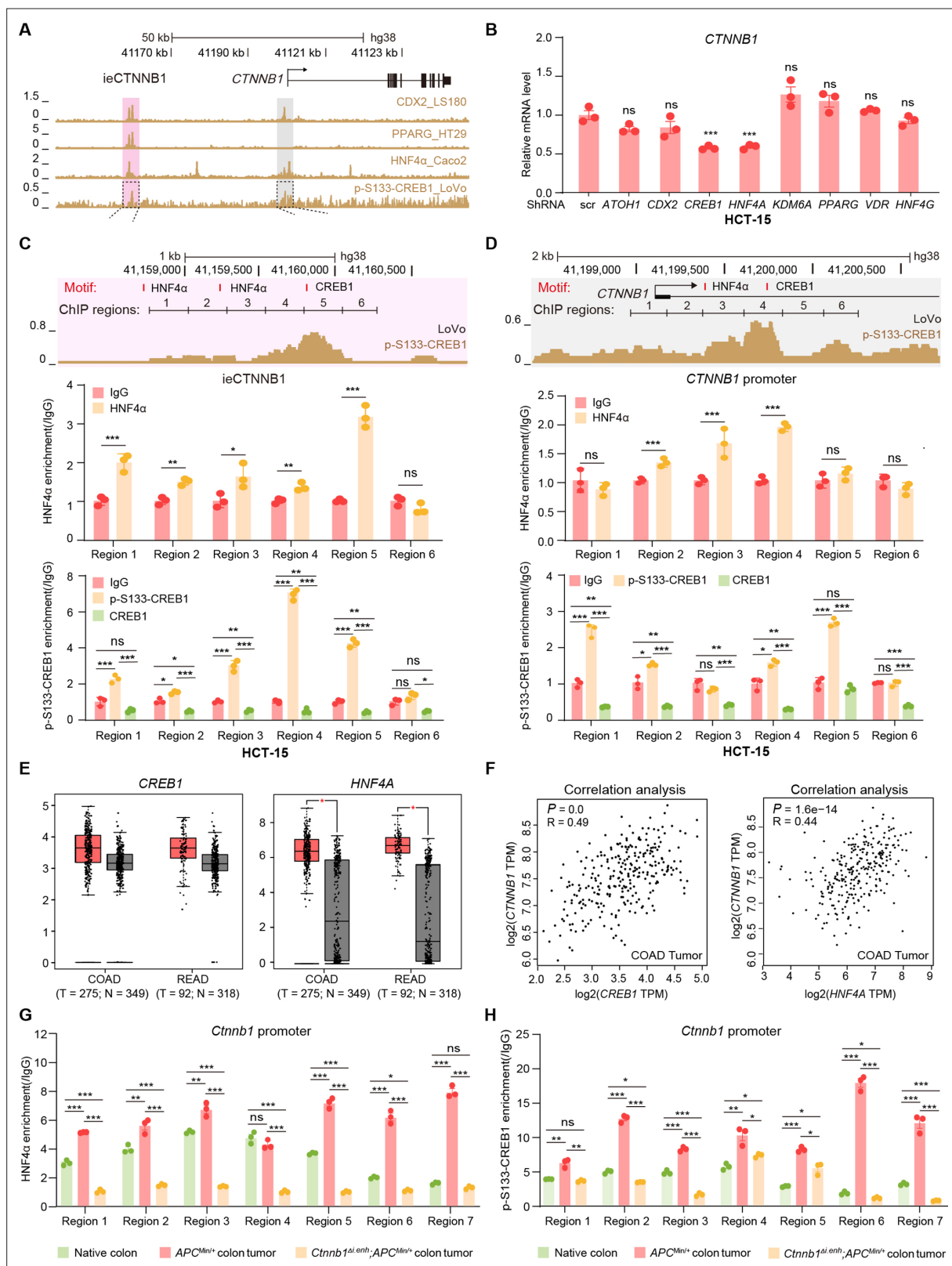


Figure 6. HNF4α and p-S133-CREB1 associate with ieCTNNB1 to regulate CTNNB1's transcription. (A) Chromatin immunoprecipitation sequencing (ChIP-seq) tracks of indicated trans-acting factors enriched at ieCTNNB1 (pink shading) and CTNNB1 promoter (gray shading) in indicated colorectal cancer cell lines. Shaded regions were enlarged in C (pink) and D (gray) respectively. (B) Quantitative reverse transcription PCR (RT-qPCR) showing relative mRNA levels of CTNNB1 in HCT-15 cells transfected with indicated shRNA-expressing plasmids for 48 hr. The expression level of CTNNB1 in

Figure 6 continued on next page

Figure 6 continued

cells transfected with scramble (scr) shRNA was set to '1'. **(C–D)** Top: schematic diagram showing the enrichment of p-S133-CREB1 at ieCTNNB1 **(C)** and CTNNB1's promoter **(D)**. Locations of HNF4 α and CREB1 binding motif sites were indicated. Middle and bottom: ChIP-qPCR showing enrichment of HNF4 α (middle), CREB1 and p-S133-CREB1 (bottom) at ieCTNNB1 **(C)**, and CTNNB1's promoter **(D)** in HCT-15 cells. Locations of ChIP regions were indicated. **(E)** Comparison of expression levels of CREB1 and HNF4A between native and tumor tissues in colon adenocarcinoma (COAD) and rectum adenocarcinoma (READ) tumors. **(F)** Correlations between the expression level of CTNNB1 and those of CREB1 or HNF4A in COAD tumors. **(G–H)** ChIP-qPCR showing enrichment of HNF4 α **(G)** and p-S133-CREB1 **(H)** at *Ctnnb1* promoter in native colon tissues of WT (n=3) mice, tumor tissues of *Apc*^{Min/+} (n=3) mice, and *Ctnnb1* ^{Δ i.enh};*Apc*^{Min/+} (n=3) mice. Quantification data are shown as means \pm SEM, statistical significance was determined using one-way ANOVA **(B)**, unpaired two-tailed Student's *t*-test **(E and F)**, and Multiple *t*-tests – one per row **(C, D, G, and H)**. **p*<0.05, ***p*<0.01, ****p*<0.001, and *****p*<0.0001. ns, not significant. R: Pearson correlation.

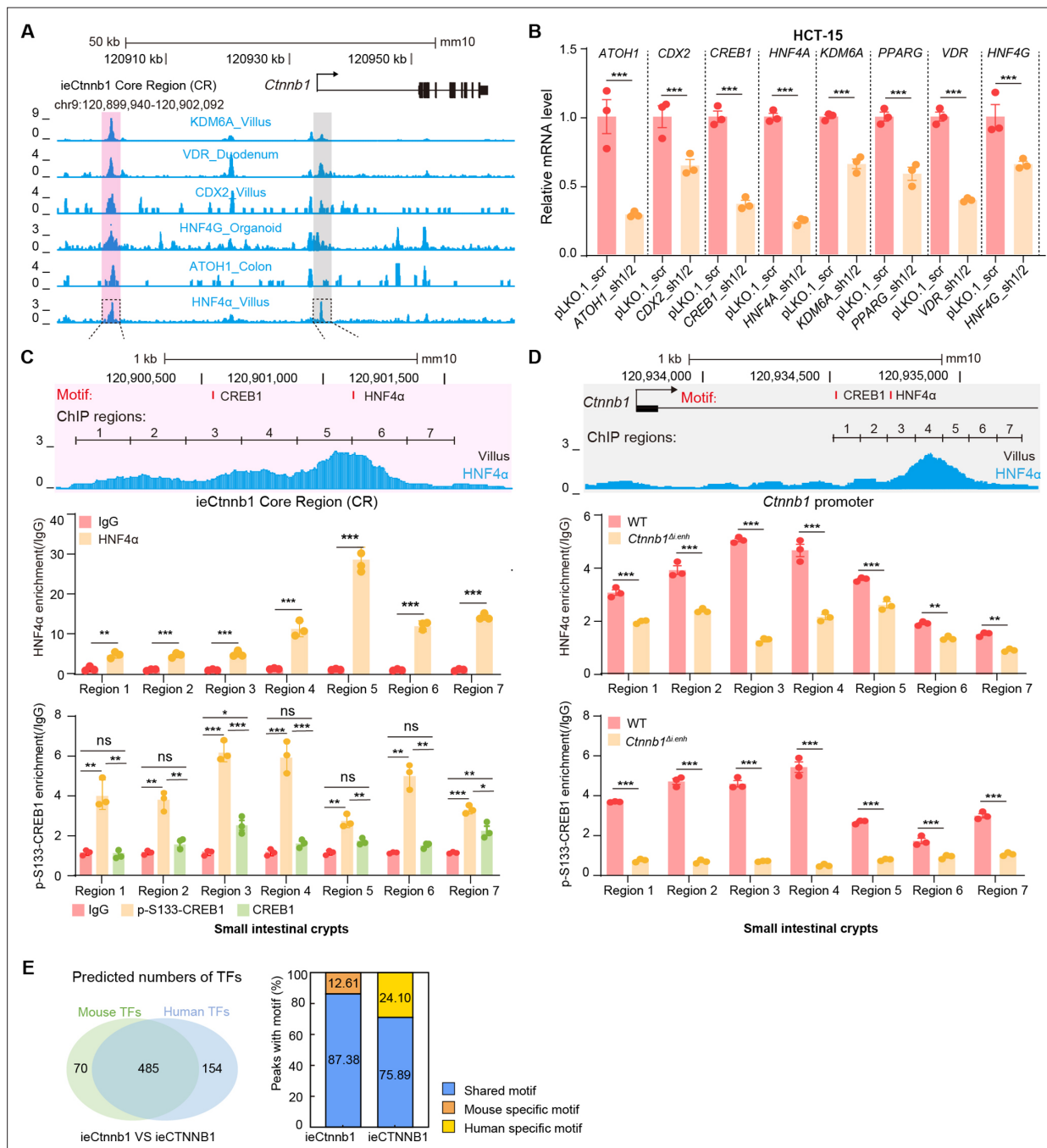


Figure 6—figure supplement 1. HNF4α and p-S133-CREB1 associate with ieCtnnb1 to regulate *Ctnnb1*'s transcription. (A) Chromatin immunoprecipitation sequencing (ChIP-seq) tracks of indicated trans-acting factors enriched at ieCtnnb1 (pink shading) and *Ctnnb1* promoter (gray shading) in mouse intestinal tissues and organoids. Shaded regions were enlarged in C (pink) and D (gray) respectively. (B) Relative mRNA levels of indicated genes in HCT-15 cells transfected with indicated shRNA-expressing plasmids for 48 hr. (C–D) Top: schematic diagram showing the enrichment of HNF4α at ieCtnnb1 (C) and *Ctnnb1*'s promoter (D). Locations of the HNF4α and CREB1 binding motif sites were indicated. Middle and bottom: ChIP-qPCR showing enrichment of HNF4α (middle), CREB1 and p-S133-CREB1 (bottom) at ieCtnnb1 (C), and *Ctnnb1*'s promoter (D) in small intestinal crypts. ChIP regions were indicated. (E) The comparison of numbers (left) and proportions (right) of species-specific and shared transcription factor binding sites within ieCtnnb1 and ieCTNNB1. Quantification data are shown as means ± SEM, statistical significance was determined using an unpaired two-tailed Student's t-test (B) and Multiple t-tests – one per row (C and D). *p<0.05, **p<0.01, ***p<0.001, and ****p<0.0001. ns, not significant.

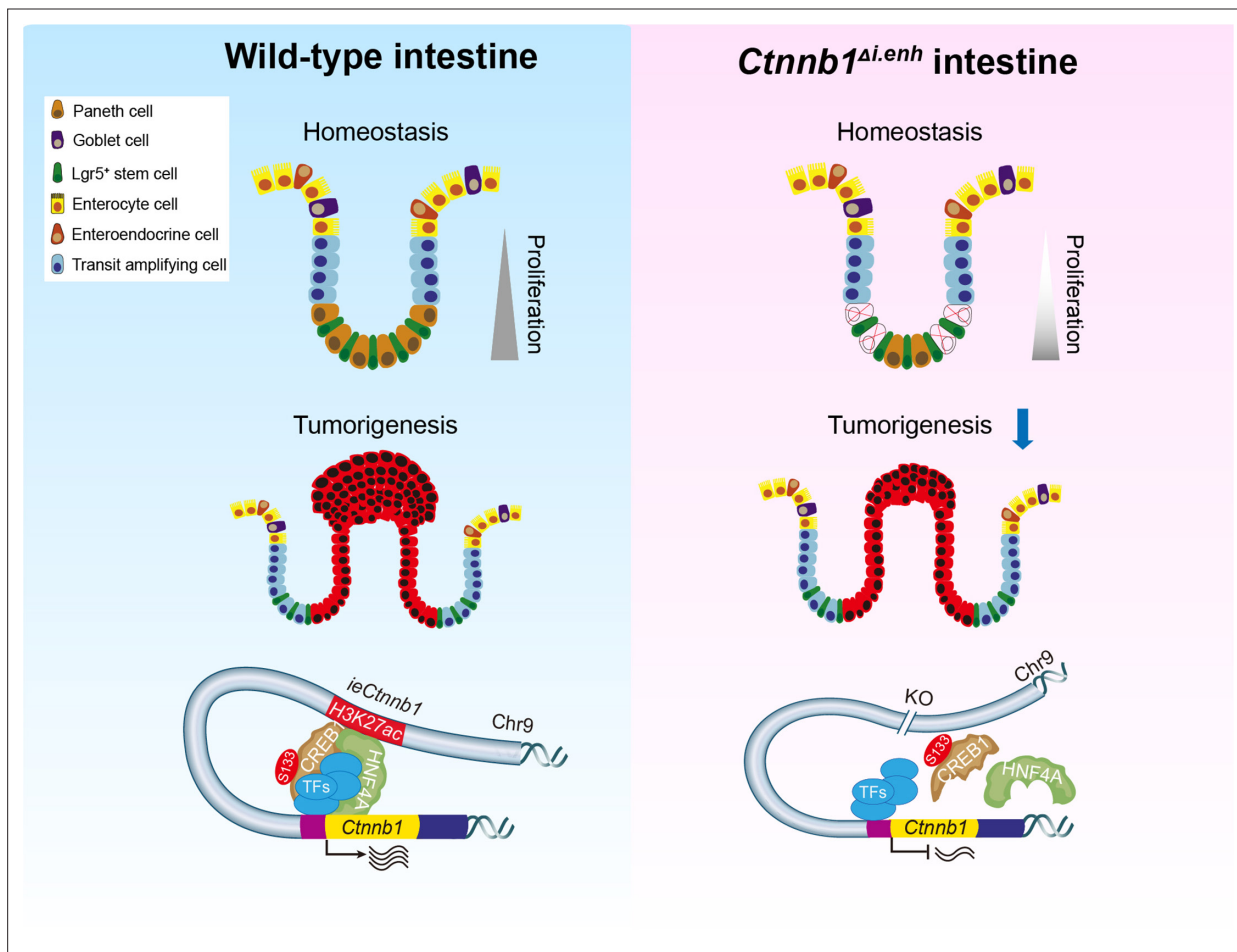


Figure 7. The working model. ieCtnnb1, the intestinal enhancer of *Ctnnb1*, balances epithelial homeostasis and tumorigenesis by transcriptionally controlling Wnt signaling dosage.